Probing the Onset of Crystallization of a Microporous Catalyst by Combined X-ray Absorption Spectroscopy and X-ray Diffraction

Gopinathan Sankar,*[a] John Meurig Thomas,*[a] Fernando Rey[a] and G. Neville Greaves[b]

[a] *Davy Faraday Research Laboratory, The Royal Institution of Great Britain, 21 Albemarle Street, London, UK W1X 4BS*

[b] *CCLRC, Daresbury Laboratory, Daresbury, Warrington, Cheshire, UK WA4 4AD*

The power of a new variant of the *in situ* combined XRA-XRD experiment (see ref. 12) is illustrated by tracking the inner shell environment and bonding of a Co^{II} ion as it changes, in the gel just prior to crystallisation, from octahedral to tetrahedral coordination, the state in which it finally appears in the microporous catalyst CoAlPO-5: the technique is widely applicable.

When transition-metal ions replace those of aluminium in the frameworks of microporous AlPOs (zeolitic aluminium phosphates) powerful solid-acid catalysts, of value in a range of petrochemical contexts, are generated.[1,2] There is much scope for 'designed' novel catalysts of this type, and considerable headway has been made experimentally[3–5] and computationally[6,7] in achieving an increase in both the number of distinct microporous frameworks and the variety of organic templates required to nucleate them. Progress in the designed synthesis of these microporous catalysts, where the active site is located in a desired, well-defined atomic environment is, however, limited by the paucity of techniques available for tracking the changing environmental path of a catalytically active ion from the precursor gel to the templated microporous solid. It has recently been shown[8,9] that the onset of crystallisation of a CoAlPO-5 and of zeolitic 4A may be quantitatively followed either by means of a position-sensitive[9] or a solid-state detector[8] (*i.e.* energy-dispersive X-ray diffraction), advantage being taken in each case of the high photon flux of synchrotron radiation. Here we report how, by a combined approach, using a capillary cell[9–11] as shown in Fig. 1, we may track changes in both the local and long-range environment during the synthesis of a crystalline catalyst MAlPO (M = Co). The merit of combining X-ray absorption (XRA) and X-ray diffraction (XRD) *in situ* to elucidate solid-state transformations[12,13] and heterogeneous catalysis[14,15] has been demonstrated previously.

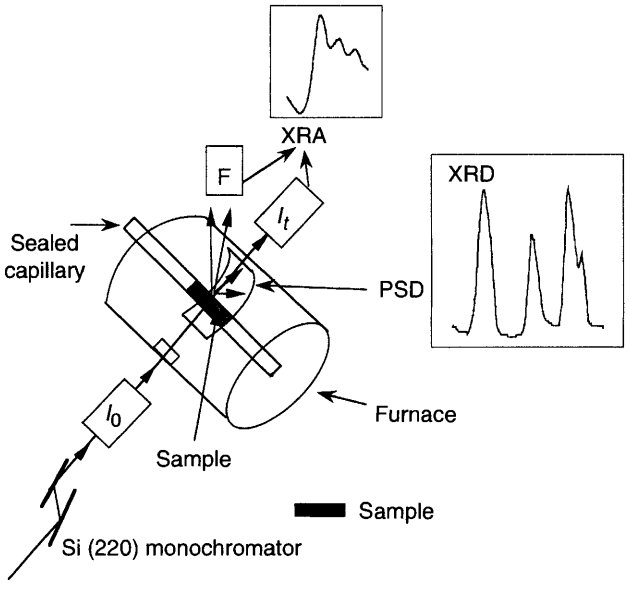

Fig. 1 Schematic diagram of the experimental setup used for the *in situ* characterisation of the synthesis of CoAlPO-5 using combined XRA/XRD technique. F denotes the fluorescence detector and PSD the position-sensitive detector (compare with Fig. 1 of ref. 12). The hypothetical outputs in the inserts are for illustrative purposes.

The composition (molar ratios) of the gel from which CoAlPO-5 crystallizes during a gradual (*ca.* 10 °C min^{-1}) increase of temperature and the order of addition, was: $1.5H_3PO_4 : 30H_2O : 0.92Al(OH)_3 : 0.08Co^{II}(MeCO_2)_2 : 0.8NEt_3$ (template). The resulting gel was stirred for 30 min to ensure homogeneity then introduced into a 1 mm diameter fused quartz capillary (10 μm wall thickness) which was sealed carefully with a thin acetylenic flame so as to avoid precipitation from local heating. The capillary crystallization cell was mounted inside a specially constructed furnace that permits the parallel collection of XRD patterns and XRA spectra (pre-, near- and extended-edge structures) of transition-metal ions in both transmission and fluorescence mode. From *ca.* 170 °C the rate of temperature rise (to *ca.* 200 °C) was 2 °C min^{-1}, during the course of which the XRD patterns were measured using a position sensitive (INEL) detector well below the cobalt K-edge (λ = 1.6714 Å). Measurements were recorded sequentially (on station 9.3 of the Daresbury Synchrotron facility which operates at 2 GeV with typical current in the range 150–250 mA), first XRD data for 220 s then XRA data for 218 s with a total of 8 min for each cycle inclusive of a 42 s dead time. Station 9.3 was equipped with a vertically focusing mirror enabling the beam to be matched to the capillary width, a Si(220) monochromator, ion chambers (for measuring the intensities of both incident and transmitted beams) and a thirteen-element (Canberra) fluorescence detector for XRA measurements. The energy range scanned (for the XRA data) was deliberately restricted to improve the statistics, time-resolution and the energy interval between data points. Full-range EXAFS scans were, however, recorded for the gel prior to and at the completion of the heat-treatment that induced crystallisation.

The peaks in the diffraction pattern (Fig. 2, top) are all assignable to the AlPO-5 structure[16] (hexagonal symmetry, space group *P6cc*, *a* = 13.7, *c* = 8.4 Å); because of its low concentration in the host no XRD peaks arise from the presence of Co^{II} in the framework. A colour change in the gel (from pink to blue) prior to onset of crystallization was apparent (in a separate experiment), strongly suggesting a change from octahedral to tetrahedral coordination. This change in local ordering is indeed borne out by the dramatic changes in X-ray absorption spectra (XRA) (Fig. 2, bottom) prior to the crystallization evident in the XRD patterns (Fig. 2, top). Comparable changes in the pre-edge peak (1s → 3d, see insert in Fig. 2, bottom) intensity accompanying conversion from octahedral to tetrahedral symmetry are well known in compounds of Ti, Cr, Mn and other transition metals.[17,18] The increased intensity of the peak and the diminution in that of the main ('white line') absorption peak are attributable to a change from O_h to T_d coordination. The former occurs because of a substantial mixing of the metal d orbital with oxygen p orbitals as well as lack of inversion symmetry in a tetrahedral environment; the latter primarily because of the degeneracy of the 4p levels in the octahedral environment and mixing of the metal 3d with the 4p orbital.[19–21] From the detailed analysis of the EXAFS data (not shown) quantitative values of coordination and bond distances (Table 1) are obtained. Changes in the Co–O

coordination number and interatomic distance during conversion from gel to crystalline CoAlPO-5 corroborate our other observations. The fact that the changes in XRA anticipate those in XRD (Fig. 2) underlines the sensitivity of XRA to changes in atomic environments on the scale of a few angstroms which clearly occur in advance of the precipitation of CoAlPO-5 crystals. From the XRD linewidths ($\Delta 2\theta$) of *ca.* 1° we estimate that crystallites are initially of the order of 50 Å in radius.

On the one hand, this experiment shows how combined XRA/XRD tracks the fate of an active ion from gel to crystal; on the other, it offers a viable, atom-specific X-ray absorption analysis of non-crystalline gels and crystalline solids when other rival techniques [such as DAFS (diffraction anomalous fine structure[21])] are inapplicable. [Whenever, as in this case, the key ion (Co^{II})] is incorporated into a framework in a random, non-ordered fashion, the DAFS approach, so powerful for ordered solids, cannot be used.] Our technique is well suited for the elucidation of atomic environments during low-temperature crystallisation (in capillaries) of a wide range of zeolites, MeAlPOs, alkali-metal suboxides (*e.g.* Rb_9O_2), alkaline earth subnitrides (*e.g.* Na_5Ba_3N) and intermetallic phases (*e.g.* K_7Cs_6).[22]

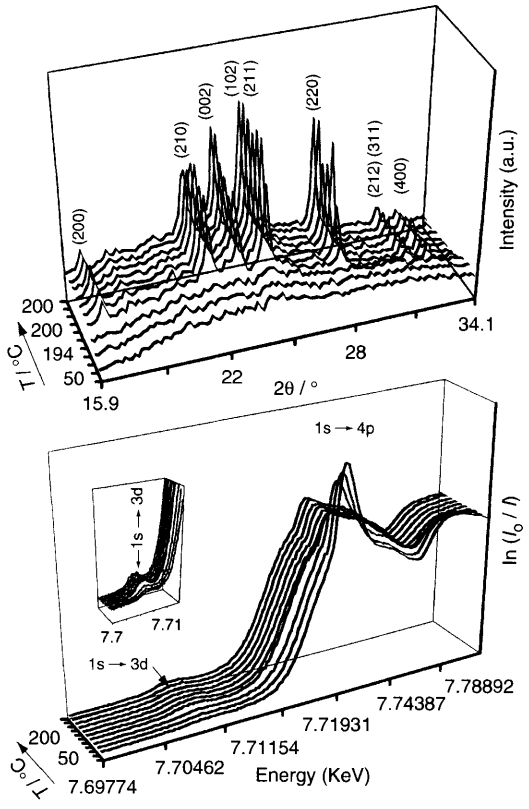

Fig. 2 XRD (top) and Co K-edge XRA patterns (bottom) recorded sequentially using the setup shown in Fig. 1. The XRD patterns track the formation of the crystalline phase from the amorphous gel while the XAS shows the change in local environment around Co^{II} during the hydrothermal synthesis of CoAlPO-5 with a typical pressure buildup of 15 bar. The insert in the lower figure shows the pre-edge peak which indicates the change in coordination of Co^{II}.

Table 1 Coordination number (n), Co–O distance (r) and Debye–Waller factor (σ) for cobalt prior to and after crystallisation[a]

	n^b	r^b/Å	σ^2/Å^2
$Co^{II}(MeCO_2)_2$	6.2	2.08	0.008
$Co^{II}(MeCO_2)_2 \cdot xH_2O$	6.4	2.08	0.008
CoAlPO (gel)	6.2	2.08	0.007
CoAlPO-5 (crystalline)	3.9	1.93	0.004

[a] $CoAl_2O_4$, normal spinel was used as a model system for estimating non-structural parameter AFAC (amplitude reduction factor). [b] Error limits for n and r are ± 10% and ± 0.02 Å, respectively.

We thank the EPSRC, EEC Human and Capital Mobility programmes (F. R.) for financial support and CCLRC, Daresbury Laboratory for the facilities.

Received, 9th October 1995; Com. 5/06657C

References

1 *Introduction to zeolitic science and practice*, ed. H. van Bekkum, E. M. Flanigen and J. C. Jansen, Elsevier, Amsterdam, 1991.
2 L. Marchese, J. Chen, J. M. Thomas, S. Coluccia and A. Zecchina, *J. Phys. Chem.*, 1994, **98**, 13350.
3 M. E. Davis, *Acc. Chem. Res.*, 1992, **26**, 111.
4 P. A. Wright, R. H. Jones, S. Natarajan, R. G. Bell, J. Chen, M. B. Hursthouse and J. M. Thomas, *J. Chem. Soc., Chem. Commun.*, 1993, 633.
5 P. A. Barrett and R. H. Jones, *J. Chem. Soc., Chem. Commun.*, 1995, 1979.
6 R. G. Bell, D. W. Lewis, P. Voigt, C. M. Freeman, J. M. Thomas and C. R. A. Catlow, *Stud. Surf. Sci. Catal.*, 1994, **84**, 2075.
7 D. W. Lewis, C. R. A. Catlow and C. M. Freeman, *J. Phys. Chem.*, 1995, **99**, 11194.
8 F. Rey, G. Sankar, J. M. Thomas, P. A. Barrett, D. W. Lewis, C. R. A. Catlow, G. N. Greaves and S. M. Clark, *Chem. Mater.*, 1995, **7**, 1435; J. S. O. Evans, R. J. Francis, D. O'Hare, S. J. Price, S. M. Clark, J. Flaherty, J. Gordon, A. Nield and C. C. Tang, *Rev. Sci. Instrum.*, 1995, **66**, 2442.
9 P. Norby, A. N. Christensen and J. C. Hanson, *Stud. Surf. Sci. Catal.*, 1994, **84**, 179.
10 B. S. Clausen, K. Grabaek, G. Steffensen, P. L. Hansen and H. Topsoe, *Catal. Lett.*, 1993, **20**, 23.
11 G. Sankar, J. M. Thomas, G. N. Greaves, F. Rey, S. M. Clark, I. Shannon, T. Maschmeyer, M. Sheehy and D. Madill, to be submitted.
12 J. W. Couves, J. M. Thomas, D. Waller, R. H. Jones, A. J. Dent, G. E. Derbyshire and G. N. Greaves, *Nature*, 1991, **345**, 465.
13 G. Sankar, J. M. Thomas, P. A. Wright, S. Natarajan, A. J. Dent, B. R. Dobson, C. A. Ramsdale, G. N. Greaves and R. H. Jones, *J. Phys. Chem.*, 1993, **97**, 9550.
14 J. M. Thomas and G. N. Greaves, *Science*, 1994, **265**, 1675.
15 G. Sankar, F. Rey, J. M. Thomas, A. Corma, G. N. Greaves, A. J. Dent and B. R. Dobson, *J. Chem. Soc., Chem. Commun.*, 1994, 2279.
16 *Atlas of Zeolitic structure types*, ed. W. M. Meier and D. H. Olson, Butterworths, 2nd edn., 1987, p. 18.
17 J. Wong, F. W. Lytle, R. P. Messmer and D. H. Maylotte, *Phys. Rev. B*, 1984, **30**, 5596.
18 N. M. D. Brown, B. McMongle and G. N. Greaves, *J. Chem. Soc., Faraday Trans. I*, 1844, **80**, 589.
19 M. Lenglet, A. D'Huysser and J. Durr, *Ann. Chim. Fr.*, 1988, **13**, 505.
20 V. Briois, C. Cartier, M. Momenteau, P. Maillard, J. Zarebowitch, E. Dartyse, A. Fontaine, G. Tourillon, P. Thuery and M. Verdaguer, *J. Chim. Phys.*, 1989, **86**, 1632.
21 I. J. Pickering, M. Sansone, J. Marsch and G. N. George, *J. Am. Chem. Soc.*, 1993, **115**, 6302.
22 A. Simon, *New trends in Materials Chemistry*, ed. C. R. A. Catlow and A. K. Cheetham, NATO ASI series, Kluwer Academic Press, Dordrecht, 1996, in the press.